



Electronically tunable low-voltage mixed-mode universal biquad filter

S. Maheshwari¹ S.V. Singh² D.S. Chauhan³

¹Department of Electronics Engineering, Z. H. College of Engineering and Technology, Aligarh Muslim University, Aligarh 202002, Uttar Pradesh, India

²Department of Electronics and Communications, Jaypee University of Information Technology, Waknaghat, Solan 173215, Himachal Pradesh, India

³Department of Electrical Engineering, Institute of Technology, Banaras Hindu University, Varanasi 221005, Uttar Pradesh, India

E-mail: sajaivir@rediffmail.com

Abstract: This study presents an electronically tunable low-voltage mixed-mode universal biquad filter. The proposed filter employs only three current controlled current conveyor trans-conductance amplifiers (CCCCTAs) and two grounded capacitors. The proposed filter can realise low pass, band pass and high pass responses in all the four possible modes, that is, voltage-mode, current-mode, trans-admittance-mode and trans-impedance-mode from the same configuration. The filter can also realise regular notch, low-pass notch, high-pass notch and all pass responses in current and trans-admittance-mode, with interconnection of relevant output currents. The filter parameters namely pole frequency, quality factor, bandwidth and filter gains can be tuned electronically. Moreover, the circuit parameters such as pole frequency and quality factor can be simultaneously current controlled without affecting bandwidth. Effects of non-idealities and parasitic are also discussed. The circuit possesses low active and passive sensitivity and can be operated at low power supply (± 1 V). The validity of the proposed filter is verified through computer simulations using PSPICE, the industry standard tool. Possible experimental setup for CCCCTA using commercial available integrated circuits is further discussed.

1 Introduction

In the past several decades there has been a great attention on designing current-mode (CM) and voltage-mode (VM) active filters using different active elements [1–17]. In some analogue signal processing applications, however, there arises need of voltage to current converter ($V-I$) interface or current to voltage converter ($I-V$) interface circuits to connect the VM circuits with the CM circuits. Thus, the trans-admittance [18] or trans-impedance mode [19] will be required in conversion between VM and CM. Therefore it is essential to have such type of filter topology that can realise the standard filter functions in CM (i.e. both input and output as current), VM (i.e. both input and output as voltage), trans-impedance mode (i.e. input as current and output as voltage) and trans-admittance mode (i.e. input as voltage and output as current) from the same topology. Such type of filter topology is called mixed-mode filter circuit. Mixed-mode filter circuits [20–29] can be classified either as multiple-input type or single-input type. However, most of these structures are multiple-input type [20–25], which can realise one standard filter function in one mode at a time. In some applications, however, simultaneous outputs of many different filter functions may be required and a very little work has been done in the domain of

single-input-type mixed-mode filters [26–29]. Comparison of previous reported single-input-type mixed-mode filters [26–29] using different active elements such as current feedback operational amplifier (CFOA), current controlled current conveyor (CCCII), fully differential current conveyor (FDCCII) are made in Table 1. A careful investigation of literature on mixed-mode filter with single-input type [26–29] (Table 1) reveals that no work is available which realises low-pass notch (LPN) and high-pass notch (HPN) along with all five standard filter functions (low pass (LP), high pass (HP), band pass (BP), regular notch (RN) and all pass (AP)) at least in any one of the four modes and provide the feature of availability of input voltage at high input impedance terminal in voltage and trans-admittance mode. This paper presents an electronically tunable low-voltage mixed-mode universal biquad filter employing only three current controlled current conveyor trans-conductance amplifiers (CCCCTAs) and two grounded capacitors. The proposed filter can realise LP, BP and HP responses in CM, trans-admittance mode, trans-impedance mode and VM. The filter can also realise RN, LPN, HPN and AP responses in current as well as trans-admittance mode, with interconnection of relevant output currents. The mixed-mode filter exhibits low active and passive sensitivities, within one in magnitude. Additionally, the filter parameters namely pole frequency, quality factor,

Table 1 Comparison of previous reported single-input-type mixed-mode filters

| Related works | No. of components used | | Functions performed | | | | Realisation from the same configuration | Orthogonal tunability of ω_o , Q and ω_o/Q | Input voltage at high input impedance |
|---------------|------------------------|-----|---------------------|--------------------|-----------------------|-----------------------|---|--|---------------------------------------|
| | Active elements | R C | Current mode | Voltage mode | Trans-admittance mode | Trans-resistance mode | | | |
| [26] | 4 CFOAs | 9 2 | LP, BP, HP, RN, AP | LP, BP, HP, RN, AP | LP, BP, HP, RN, AP | LP, BP, HP, RN, AP | no | no | no |
| [27] | 4 CCCIIIs | – 2 | LP, BP, HP, RN, AP | BP, LP | LP, BP, HP, RN, AP | BP, LP | yes | yes | no |
| [28] | 5 MCCCIIIs | – 2 | LP, BP, HP | LP, BP, HP | LP, BP, HP | LP, BP, HP | yes | yes | no |
| [29] | 1 FDCCII | 3 2 | BP, HP | LP, BP, HP, RN, AP | BP, HP | LP, BP, HP, RN, AP | yes | yes | no |
| present work | 3 CCCCTAs | – 2 | LP, BP, HP, RN, AP | LP, BP, HP | LP, BP, HP, RN, AP | LP, BP, HP | yes | yes | yes |

bandwidth and filter gains can be tuned electronically. Moreover, the circuit parameters such as pole frequency and quality factor can be simultaneously controlled electronically without affecting bandwidth. The performances of the proposed circuit are illustrated by PSPICE simulations.

2 CCCCTA descriptions

CCCCTA is relatively new active element [30] and has received considerable attention as CM active element, because its trans-conductance and parasitic resistance can be adjusted electronically, hence it does not need a resistor in practical applications. This device can be operated in both current and VMs, providing flexibility. In addition, it can offer the advantages associated with CM active elements. For instance, a CM commercially available chip AD844 has slew rate of around 2000 V/ μ s and a unity gain bandwidth of 60 MHz. All these advantages together with its CM operation make the CCCCTA a promising choice for realising active filters [30]. The CCCCTA properties can be described by the following equations

$$V_{Xi} = V_{Yi} + I_{Xi}R_{Xi}, \quad I_{Zi} = I_{Xi}, \quad I_{-Zi} = -I_{Xi} \quad (1)$$

$$I_{\pm O} = \pm g_{mi}V_{Zi}$$

where R_{Xi} and g_{mi} are the parasitic resistance at X terminal and trans-conductance of the i th CCCCTA, respectively. R_{Xi} and g_{mi} depend upon the biasing currents I_{Bi} and I_{Si} of the CCCCTA, respectively. The schematic symbol of CCCCTA is illustrated in Fig. 1. For BJT model of CCCCTA [30]

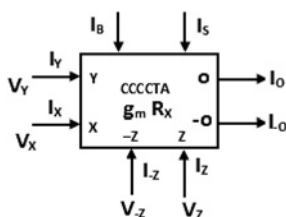


Fig. 1 CCCCTA symbol

shown in Fig. 2, R_{Xi} and g_{mi} can be expressed as

$$R_{Xi} = \frac{V_T}{2I_{Bi}} \quad \text{and} \quad g_{mi} = \frac{I_{Si}}{2V_T} \quad (2)$$

3 Proposed filter circuit

The proposed mixed-mode universal biquad filter is shown in Fig. 3. It is based on three CCCCTAs and two grounded capacitors. If $V_{in} = 0$ and I_{in} is taken as input signal, the proposed circuit as shown in Fig. 3 yields the four current transfer functions at current outputs $I_1(s)$, $I_2(s)$, $I_3(s)$ and $I_4(s)$ and three trans-impedance-mode transfer functions at voltage outputs $V_1(s)$, $V_2(s)$ and $V_3(s)$, as described in Table 2. The four current transfer functions obtained are

$$\frac{I_1(s)}{I_{in}(s)} = \frac{s^2 C_1 C_2 R_{X1} R_{X2}}{s^2 C_1 C_2 R_{X1} R_{X2} + s C_2 R_{X3} + g_{m2} R_{X3}} \quad (3)$$

$$\frac{I_2(s)}{I_{in}(s)} = \frac{g_{m2} R_{X3}}{s^2 C_1 C_2 R_{X1} R_{X2} + s C_2 R_{X3} + g_{m2} R_{X3}} \quad (4)$$

$$\frac{I_3(s)}{I_{in}(s)} = \frac{-s C_2 g_{m1} R_{X2} R_{X3}}{s^2 C_1 C_2 R_{X1} R_{X2} + s C_2 R_{X3} + g_{m2} R_{X3}} \quad (5)$$

$$\frac{I_4(s)}{I_{in}(s)} = \frac{s^2 C_1 C_2 R_{X2} R_{X3}}{s^2 C_1 C_2 R_{X1} R_{X2} + s C_2 R_{X3} + g_{m2} R_{X3}} \quad (6)$$

Equations (3) and (4) represent the current transfer functions of unity gain HP and LP filter function, respectively. Equations (5) and (6) represent the current transfer functions of inverted BP and HP filter function with electronically controlled gain, respectively, and can be formulated by

$$H_3 = g_{m1} R_{X2} = \frac{I_{S1}}{4I_{B2}} \quad \text{and} \quad H_4 = \frac{R_{X3}}{R_{X1}} = \frac{I_{B1}}{I_{B3}} \quad (7)$$

It can be seen that the filter circuit can simultaneously realise the LP, BP and two HP transfer functions (one having unity gain and other having variable gain) at current outputs of $I_2(s)$, $I_3(s)$, $I_1(s)$ and $I_4(s)$, respectively. The RN transfer function can be easily obtained by simply connecting $I_1(s)$ and $I_2(s)$ together. The AP transfer function

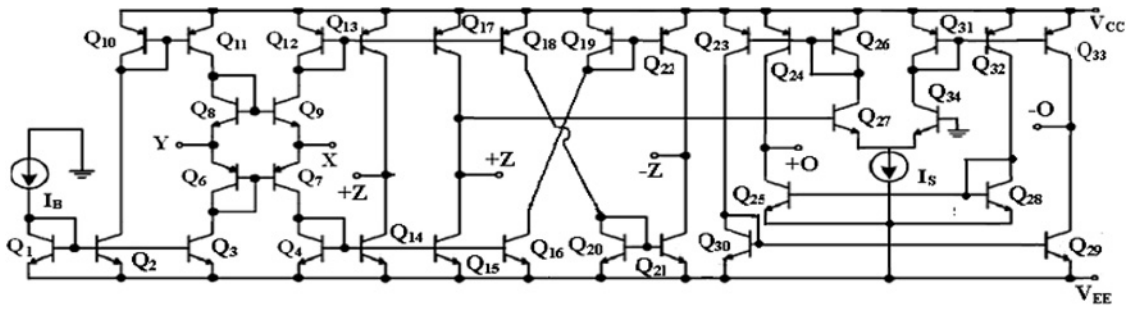


Fig. 2 Internal topology of CCCCTA

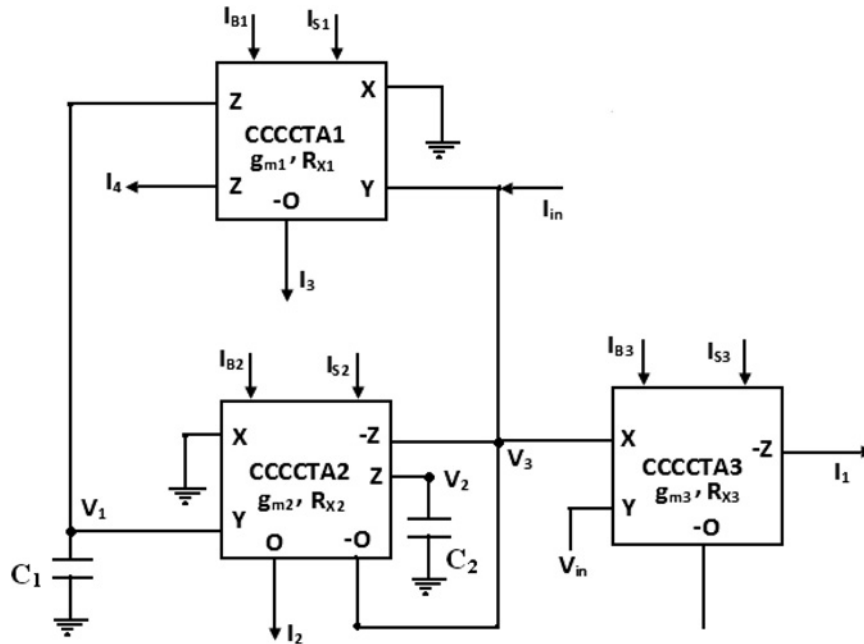


Fig. 3 Proposed mixed-mode universal biquad filter

Table 2 Input conditions and various functions realised

| Input conditions | $V_{in} = 0, I_{in}$ is input signal | | $I_{in} = 0, V_{in}$ is input signal | |
|------------------|---|----------------------|---|--------------|
| | Current mode | Trans-impedance mode | Trans-admittance mode | Voltage mode |
| HP | $I_1(s)$ and $I_4(s)$ | $V_3(s)$ | $I_1(s)$ | $V_3(s)$ |
| LP | $I_2(s)$ | $V_2(s)$ | $I_2(s)$ | $V_2(s)$ |
| BP | $I_3(s)$ | $V_1(s)$ | $I_3(s)$ and $I_2(s) + I_4(s)$ | $V_1(s)$ |
| RN | $I_1(s) + I_2(s)$ | | $I_1(s) + I_2(s)$, for $I_{B1} = I_{B3}$ | |
| AP | $I_1(s) + I_2(s) + I_3(s)$, for $I_{S1} = 4I_{B2}$ | | $I_1(s) + I_2(s) + I_3(s)$, for $I_{S1} = 4I_{B2}$ and $I_{B1} = I_{B3}$ | |
| LPN | $I_2(s) + I_4(s)$, for $I_{B1} < I_{B3}$ | | $I_1(s) + I_2(s)$, for $I_{B1} < I_{B3}$ | |
| HPN | $I_2(s) + I_4(s)$, for $I_{B1} > I_{B3}$ | | $I_1(s) + I_2(s)$, for $I_{B1} > I_{B3}$ | |

can also be easily obtained by simply connecting $I_1(s)$, $I_2(s)$ and $I_3(s)$ together with $I_{S1} = 4I_{B2}$. Moreover, LPN and HPN filter functions can also be realised by simply connecting $I_2(s)$ and $I_4(s)$ together by maintaining the conditions $I_{B1} < I_{B3}$ and $I_{B1} > I_{B3}$, respectively. In addition to above current transfer functions, three trans-impedance-mode transfer functions (BP, LP and HP) are simultaneously obtained as

$$\frac{V_1(s)}{I_{in}(s)} = \frac{sC_2R_{X2}R_{X3}}{s^2C_1C_2R_{X1}R_{X2} + sC_2R_{X3} + g_{m2}R_{X3}} \quad (8)$$

$$\frac{V_2(s)}{I_{in}(s)} = \frac{R_{X3}}{s^2C_1C_2R_{X1}R_{X2} + sC_2R_{X3} + g_{m2}R_{X3}} \quad (9)$$

$$\frac{V_3(s)}{I_{in}(s)} = \frac{s^2C_1C_2R_{X1}R_{X2}R_{X3}}{s^2C_1C_2R_{X1}R_{X2} + sC_2R_{X3} + g_{m2}R_{X3}} \quad (10)$$

Similarly, if $I_{in} = 0$, and V_{in} is taken as the input signal, the proposed circuit as shown in Fig. 3 yields the four trans-admittance-mode transfer functions at current outputs $I_1(s)$, $I_2(s)$, $I_3(s)$ and $I_4(s)$ and three VM transfer functions

at voltage outputs $V_1(s)$, $V_2(s)$ and $V_3(s)$, as described in Table 2.

Three VM transfer functions obtained are

$$\frac{V_1(s)}{V_{in}(s)} = \frac{sC_2R_{X2}}{s^2C_1C_2R_{X1}R_{X2} + sC_2R_{X3} + g_{m2}R_{X3}} \quad (11)$$

$$\frac{V_2(s)}{V_{in}(s)} = \frac{1}{s^2C_1C_2R_{X1}R_{X2} + sC_2R_{X3} + g_{m2}R_{X3}} \quad (12)$$

$$\frac{V_3(s)}{V_{in}(s)} = \frac{s^2C_1C_2R_{X1}R_{X2}}{s^2C_1C_2R_{X1}R_{X2} + sC_2R_{X3} + g_{m2}R_{X3}} \quad (13)$$

The four trans-admittance-mode transfer functions in this case are

$$\frac{I_1(s)}{V_{in}(s)} = \frac{s^2C_1C_2R_{X2}}{s^2C_1C_2R_{X1}R_{X2} + sC_2R_{X3} + g_{m2}R_{X3}} \quad (14)$$

$$\frac{I_2(s)}{V_{in}(s)} = \frac{g_{m2}}{s^2C_1C_2R_{X1}R_{X2} + sC_2R_{X3} + g_{m2}R_{X3}} \quad (15)$$

$$\frac{I_3(s)}{V_{in}(s)} = \frac{-sC_2R_{X2}g_{m1}}{s^2C_1C_2R_{X1}R_{X2} + sC_2R_{X3} + g_{m2}R_{X3}} \quad (16)$$

$$\frac{I_4(s)}{V_{in}(s)} = \frac{-(C_2s + g_{m2})}{s^2C_1C_2R_{X1}R_{X2} + sC_2R_{X3} + g_{m2}R_{X3}} \quad (17)$$

Equations (11)–(13) represent the voltage transfer functions of BP, LP and HP filter function, respectively. Equations (14) and (15) represent HP and LP filter functions and (16) represents inverted BP filter function in trans-admittance mode. Additional responses in trans-admittance mode namely RN and AP can be easily obtained by connecting I_1 and I_2 (by keeping $I_{B1} = I_{B3}$) for RN and I_1 , I_2 and I_3 (by keeping $I_{B1} = I_{B3}$ and $I_{S1} = 4I_{B2}$) for AP response. LPN and HPN can also be easily obtained by connecting I_1 and I_2 , together and maintaining the condition $I_{B1} < I_{B3}$ and $I_{B1} > I_{B3}$, respectively. Another inverted BP response in trans-admittance form can also be obtained by simply joining I_2 and I_4 . The pole frequency (ω_o), the quality factor (Q) and bandwidth (BW) ω_o/Q of filter in each mode can be expressed as

$$\omega_o = \left(\frac{g_{m2}R_{X3}}{C_1C_2R_{X1}R_{X2}} \right)^{(1/2)}, \quad Q = \left(\frac{C_1g_{m2}R_{X1}R_{X2}}{C_2R_{X3}} \right)^{(1/2)}$$

and $BW = \frac{\omega_o}{Q} = \frac{R_{X3}}{C_1R_{X1}R_{X2}}$ (18)

Substituting intrinsic resistances as depicted in (2), it yields

$$\omega_o = \frac{1}{V_T} \left(\frac{I_{B1}I_{B2}I_{S2}}{I_{B3}C_1C_2} \right)^{(1/2)}, \quad Q = \frac{1}{2} \left(\frac{C_1I_{S2}I_{B3}}{C_2I_{B1}I_{B2}} \right)^{(1/2)} \quad (19)$$

From (19), by maintaining the ratio I_{B3} and I_{S2} to be constant, it can be remarked that the quality factor can be adjusted by I_{B3} and I_{S2} without affecting the pole frequency. In

addition, bandwidth (BW) of the system can be expressed by

$$BW = \frac{\omega_o}{Q} = \frac{2}{V_T} \frac{I_{B1}I_{B2}}{I_{B3}C_1} \quad (20)$$

Equation (20) shows that the bandwidth can be controlled by either I_{B1} or I_{B2} linearly. It can also be controlled by I_{B3} . From (19) and (20), it is clear that parameters ω_o and Q can be simultaneously controlled electronically by adjusting bias current I_{S2} without disturbing parameter ω_o/Q .

4 Influence of CCCCTA parasitic elements and non-idealities

4.1 Influence of CCCCTA parasitic elements

In this section, the performance of the proposed mixed-mode filter circuit in the presence of various parasitic elements in CCCCTA is to be considered. A practical CCCCTA, like any active element, shows various ports parasitic. These are port Y parasitic in the form of R_{Yi}/C_{Yi} , port Z parasitic in the form of R_{Zi}/C_{Zi} , port O parasitic in the form of R_{Oi}/C_{Oi} and port X parasitic in the form of L_{Xi} in series to R_{Xi} where $i = 1, 2, 3$ and indicate i th CCCCTA. The effects of these parasitic elements on filter response depend strongly upon the circuit topology. In the presence of these parasitic elements, the proposed mixed-mode filter as shown in Fig. 3 can be transformed to Fig. 4. The inductance (L_{Xi}) is ignored as it affects the response at very high frequency. Assuming that $\min(C_1, C_2) \gg$ parasitic capacitances (C_{Yi} , C_{Zi} and C_{Oi}), we can obtain that

$$Z_1 = (C_1 // C_{Y2} // C_{Z1}) // (R_{Y2} // R_{Z1}) = \frac{R_a}{(1 + sC_1R_a)} \quad (21)$$

$$Z_2 = (C_2 // C_{Z2}) // R_{Z2} = \frac{R_{Z2}}{(1 + sC_2R_{Z2})} \quad (22)$$

$$Z_3 = (C_{O2} // C_{Z2} // C_{Y1}) // (R_{O2} // R_{Z2} // R_{Y1}) = \frac{R_b}{(1 + sC_bR_b)} \quad (23)$$

where

$$R_a = R_{Y2} // R_{Z1} = \frac{R_{Y2}R_{Z1}}{(R_{Y2} + R_{Z1})}, \quad R_b = (R_{O2} // R_{Z2} // R_{Y1})$$

$$\text{and } C_b = (C_{O2} // C_{Z2} // C_{Y1}) \quad (24)$$

On reanalysing the proposed mixed-mode filter, taking into account the above parasitic effects, we obtain the following CM transfer functions at current outputs $I_1(s)$, $I_2(s)$, $I_3(s)$ and $I_4(s)$ and trans-impedance-mode transfer functions at voltage outputs $V_1(s)$, $V_2(s)$ and $V_3(s)$, by applying $V_{in} = 0$ and I_{in} as input current (see (25)–(31)).

$$\frac{I_1(s)}{I_{in}(s)} = \frac{R_{X1}R_{X2}Z_3}{Z_1Z_3R_{X3} + R_{X1}R_{X2}Z_3 + g_{m2}R_{X3}Z_1Z_2Z_3 + R_{X1}R_{X2}R_{X3}} = \frac{R_{X1}R_{X2}R_b(1 + sC_1R_a)(1 + sC_2R_{Z2})}{D(s)} \quad (25)$$

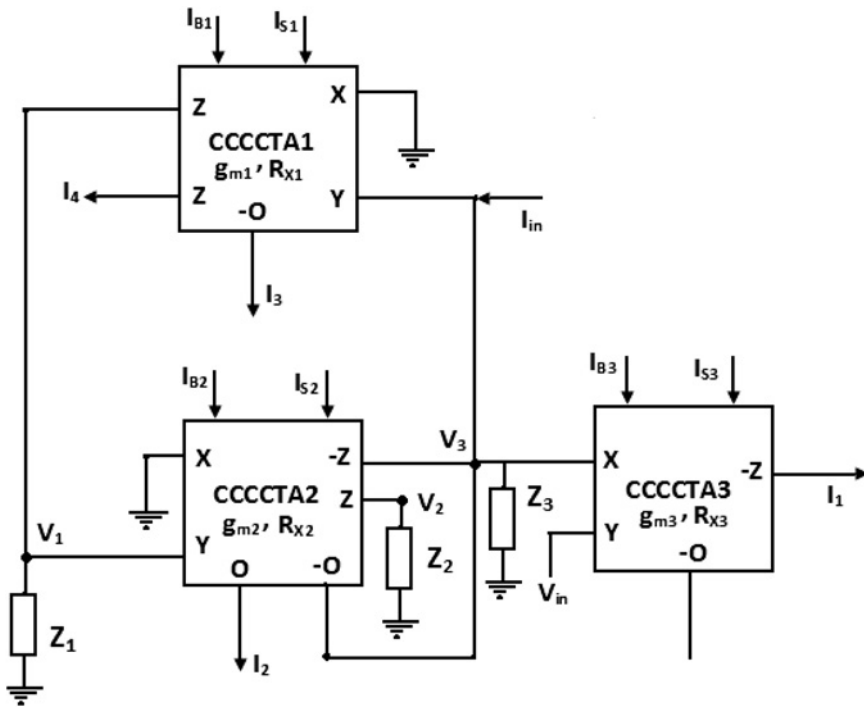


Fig. 4 Proposed mixed-mode universal biquad filter including the parasitic elements of the CCCCTA

where

$$D(s) = ms^2 + ns + p \quad (32) \quad n = R_{X1}R_{X2}R_{X3}(C_2R_{Z2} + C_bR_b + C_1R_a) + R_{X1}R_{X2}R_b(C_2R_{Z2} + C_1R_a) + R_{X3}R_aR_bR_{Z2}C_2 \quad (34)$$

m , n and p can be expressed by (33)–(35)

$$m = R_{X1}R_{X2}R_aR_bC_1(R_{Z2}C_2 + C_bR_{X3}) + R_{X1}R_{X2}R_{X3}R_{Z2}C_2(C_1R_a + C_bR_b) + sR_{X1}R_{X2}R_{X3}R_aR_bR_{Z2}C_1C_2C_b \quad (33) \quad p = R_aR_bR_{X3} + R_{X1}R_{X2}R_b + R_{X1}R_{X2}R_{X3} + g_{m2}R_{Z2}R_aR_bR_{X3} \quad (35)$$

The pole frequency and quality factor of the proposed filter in

$$\frac{I_2(s)}{I_{in}(s)} = \frac{g_{m2}R_{X3}Z_1Z_2Z_3}{Z_1Z_3R_{X3} + R_{X1}R_{X2}Z_3 + g_{m2}R_{X3}Z_1Z_2Z_3 + R_{X1}R_{X2}R_{X3}} = \frac{g_{m2}R_{X3}R_aR_bR_{Z2}}{D(s)} \quad (26)$$

$$\frac{I_3(s)}{I_{in}(s)} = \frac{-g_{m1}R_{X2}R_{X3}Z_1Z_3}{Z_1Z_3R_{X3} + R_{X1}R_{X2}Z_3 + g_{m2}R_{X3}Z_1Z_2Z_3 + R_{X1}R_{X2}R_{X3}} = \frac{-g_{m1}R_{X2}R_{X3}R_aR_b(1 + sC_2R_{Z2})}{D(s)} \quad (27)$$

$$\frac{I_4(s)}{I_{in}(s)} = \frac{R_{X2}R_{X3}Z_3}{Z_1Z_3R_{X3} + R_{X1}R_{X2}Z_3 + g_{m2}R_{X3}Z_1Z_2Z_3 + R_{X1}R_{X2}R_{X3}} = \frac{R_{X2}R_{X3}R_b(1 + sC_1R_a)(1 + sC_2R_{Z2})}{D(s)} \quad (28)$$

$$\frac{V_1(s)}{I_{in}(s)} = \frac{R_{X3}R_{X2}Z_3Z_1}{Z_1Z_3R_{X3} + R_{X1}R_{X2}Z_3 + g_{m2}R_{X3}Z_1Z_2Z_3 + R_{X1}R_{X2}R_{X3}} = \frac{R_{X2}R_{X3}R_aR_b(1 + sC_2R_{Z2})}{D(s)} \quad (29)$$

$$\frac{V_2(s)}{I_{in}(s)} = \frac{R_{X3}Z_1Z_2Z_3}{Z_1Z_3R_{X3} + R_{X1}R_{X2}Z_3 + g_{m2}R_{X3}Z_1Z_2Z_3 + R_{X1}R_{X2}R_{X3}} = \frac{R_{X3}R_aR_bR_{Z2}}{D(s)} \quad (30)$$

$$\frac{V_3(s)}{I_{in}(s)} = \frac{R_{X1}R_{X2}R_{X3}Z_3}{Z_1Z_3R_{X3} + R_{X1}R_{X2}Z_3 + g_{m2}R_{X3}Z_1Z_2Z_3 + R_{X1}R_{X2}R_{X3}} = \frac{R_{X1}R_{X2}R_{X3}R_b(1 + sC_1R_a)(1 + sC_2R_{Z2})}{D(s)} \quad (31)$$

the presence of parasitic elements are changed to

$$\omega_o^* = \omega_o \sqrt{\frac{1 + \frac{1}{g_{m2}R_{Z2}} + \frac{R_{X1}R_{X2}}{R_a R_{Z2} g_{m2} R_{X3}} + \frac{R_{X1}R_{X2}}{R_a R_b R_{Z2} g_{m2}}}{1 + \frac{R_{X3} C_b}{R_{Z2} C_2} + \frac{R_{X3}}{R_b} + \frac{R_{X3} C_b}{R_a C_1} + sR_{X3} C_b}} \quad (36)$$

(see (37))

where ω_o and Q are pole frequency and quality factor of the proposed filter, respectively, in ideal case and given by the expressions in (18). For the value of C_b smaller than 5 pf and that of R_a , R_b and R_{Z2} are larger than 100 K Ω , so C_1 , C_2 , R_{X1} , R_{X2} and R_{X3} are chosen under the following relations: $C_b \ll \min(C_1, C_2)$ and $R_a, R_b, R_{Z2} \gg \max(R_{X1}, R_{X2}, R_{X3})$. Therefore we can obtain

$$\omega_o^* = \omega_o \sqrt{\frac{1}{1 + \omega^2 R_{X3}^2 C_b^2}} \quad (38)$$

$$Q^* = Q \sqrt{1 + \omega^2 R_{X3}^2 C_b^2} \quad (39)$$

From (38) and (39), it is clear that when considering the effects of parasitic elements, the pole frequency is less than the one, in ideal condition, namely $\omega_o^* < \omega_o$ and the quality factor is higher than that in the ideal one ($Q^* > Q$). If $\omega R_{X3} C_b \ll 1$, the effects of parasitic elements of CCCCTA can be ignored.

4.2 Influence of non-idealities

Taking the non-idealities of CCCCTA into account, the relationship of the terminal voltages and currents can be rewritten as follows

$$\begin{aligned} V_{Xi} &= \beta_i V_{Yi} + I_{Xi} R_{Xi}, & I_{Zi} &= \alpha_{pi} I_{Xi} \\ I_{-Zi} &= -\alpha_{ni} I_{Xi}, & I_{\pm O} &= \pm \gamma_i g_{mi} V_{Zi} \end{aligned} \quad (40)$$

where $\beta_i = 1 - \varepsilon_{vi}$ and ε_{vi} ($|\varepsilon_{vi}| \ll 1$) represents the voltage tracking error from Y to X terminal, and $\alpha_{pi} = 1 - \varepsilon_{pi}$ and ε_{pi} ($|\varepsilon_{pi}| \ll 1$) represents the current tracking error from X to $+Z$ terminal and $\alpha_{ni} = 1 - \varepsilon_{ni}$ and ε_{ni} ($|\varepsilon_{ni}| \ll 1$) represents the current tracking error from X to $-Z$ terminal and γ_i is the trans-conductance inaccuracy factor from Z to O terminal. The non-ideal analysis of the proposed filter in Fig. 3 yields the denominator of the transfer functions in each mode as

$$\begin{aligned} D(s) &= s^2 C_1 C_2 R_{X1} R_{X2} + \alpha_{p1} \alpha_{n2} \beta_1 \beta_2 s C_2 R_{X3} \\ &+ \alpha_{p1} \alpha_{p2} \beta_1 \beta_2 \gamma_2 g_{m2} R_{X3} \end{aligned} \quad (41)$$

In this case, the ω_o and Q are changed to

$$\begin{aligned} \omega_o &= \left(\frac{\alpha_{p1} \alpha_{p2} \beta_1 \beta_2 \gamma_2 g_{m2} R_{X3}}{C_1 C_2 R_{X1} R_{X2}} \right)^{(1/2)} \\ Q &= \frac{1}{\alpha_{n2}} \left(\frac{\alpha_{p2} \gamma_2 C_1 g_{m2} R_{X1} R_{X2}}{\alpha_{p1} \beta_1 \beta_2 C_2 R_{X3}} \right)^{(1/2)} \end{aligned} \quad (42)$$

The active and passive sensitivities of the proposed circuit, as shown in Fig. 3, can be found as

$$S_{C_1, C_2, R_{X1}, R_{X2}}^{\omega_o} = -\frac{1}{2}, \quad S_{g_{m2}, R_{X3}}^{\omega_o} = \frac{1}{2} \quad (43)$$

$$S_{\alpha_{p1}, \alpha_{p2}, \beta_1, \beta_2, \gamma_2}^{\omega_o} = \frac{1}{2}, \quad S_{\alpha_{n2}, \alpha_{n3}, \gamma_1, \gamma_3, \beta_3, g_{m1}, g_{m3}}^{\omega_o} = 0$$

$$S_{R_{X3}, C_2, \alpha_{p1}, \beta_1, \beta_2}^Q = -\frac{1}{2}, \quad S_{R_{X1}, R_{X2}, g_{m2}, C_1, \alpha_{p2}, \gamma_2}^Q = \frac{1}{2} \quad (44)$$

$$S_{\alpha_{n2}}^Q = -1, \quad S_{\alpha_{n3}, \gamma_1, \gamma_3, \beta_3, g_{m1}, g_{m3}}^Q = 0$$

From (43) and (44), it can be observed that all the sensitivities are low and within one in magnitude.

5 Simulation results

To verify the theoretical analysis of the proposed filter circuit in Fig. 3, PSPICE simulation had been used. In the simulation, the CCCCTA was implemented using BJT model as shown in Fig. 2, with the transistor model of HFA3096 mixed transistors arrays [31]. The PSPICE model parameters are given in Table 3. Using the PSPICE simulation, the -3 dB bandwidths of the CCCCTA from port Z to port X (I_Z/I_X) and from port O to port X (I_O/I_X) were determined as 300 and 253.4 MHz, respectively. To obtain $f_o = \omega_o/2\pi = 1.134$ MHz at $Q = 1$, the active and passive components were chosen as $I_{B1} = I_{B2} = I_{B3} = 60 \mu\text{A}$, $I_{S1} = I_{S3} = 220 \mu\text{A}$, $I_{S2} = 240 \mu\text{A}$ and $C_1 = C_2 = 0.65$ nf. Fig. 5 shows the simulated gain responses of the LP, HP, BP, RN and AP of current and trans-admittance-mode filter of Fig. 3. Fig. 6 shows the simulated gain responses of the LP, BP and HP of voltage and trans-impedance-mode filter of Fig. 3. Fig. 7 shows the current gain and phase response of AP filter. The supply voltages were $V_{DD} = -V_{SS} = 1$ V. The simulation results show the simulated pole frequency as 1.06 MHz, that is, approximately 6.5% in error with the theoretical value. This discrepancy is quite justifiable with the discussion in Section 4. The power dissipation of the proposed circuit for the above design values was found as 4.84 mW. Table 4 shows the calculated values of I_{B3} (R_{X3}) and corresponding ideal and simulated values of pole frequency. It is observed that when R_{X3} is large (I_{B3} is small), the simulated pole frequency is lower than the one in ideal condition. When R_{X3} is small ($= 216 \Omega$), the simulated pole frequency is close to the one in ideal condition. Figs. 8 and 9 show the gain response of CM HPN and LPN, respectively. LPN was

$$Q^* = Q \frac{\sqrt{\left(1 + \frac{1}{g_{m2}R_{Z2}} + \frac{R_{X1}R_{X2}}{R_a R_{Z2} g_{m2} R_{X3}} + \frac{R_{X1}R_{X2}}{R_a R_b R_{Z2} g_{m2}}\right) \left(1 + \frac{R_{X3} C_b}{R_{Z2} C_2} + \frac{R_{X3}}{R_b} + \frac{R_{X3} C_b}{R_a C_1} + sR_{X3} C_b\right)}}{\left(1 + \frac{R_{X1}R_{X2} C_1}{R_{X3} R_{Z2} C_2} + \frac{R_{X1}R_{X2}}{R_{X3} R_a} + \frac{R_{X1}R_{X2} C_b}{R_a R_{Z2} C_2} + \frac{R_{X1}R_{X2} C_1}{R_b R_{Z2} C_2} + \frac{R_{X1}R_{X2}}{R_a R_b}\right)} \quad (37)$$

Table 3 SPICE model parameters of HFA3096 mixed transistors arrays

| | |
|------------|---|
| .model npn | $I_s = 1.80E - 17, X_{ti} = 3.20, E_g = 1.167, V_{af} = 151.0, B_f = 1.10E + 02, N_e = 2.000, I_{se} = 1.03E - 16, I_{Kf} = 1.18E - 02, X_{tb} = 2.15, B_r = 8.56E - 02, I_{K_r} = 1.18E - 02, R_c = 1.58E + 02, C_{jc} = 2.44E - 14, M_{jc} = 0.350, V_{jc} = 0.633, C_{je} = 5.27E - 14, M_{je} = 0.350, V_{je} = 1.250, T_r = 5.16E - 08, T_f = 2.01E - 11, I_{tf} = 2.47E - 02, V_{tf} = 6.62, X_{tf} = 25.98, R_b = 8.11E + 02, N_e = 2, I_{sc} = 0, F_c = .5$ |
| .model npn | $I_s = 8.40E - 18, X_{ti} = 3.67, E_g = 1.145, V_{af} = 57.0, B_f = 9.55E + 01, N_e = 2.206, I_{se} = 3.95E - 16, I_{Kf} = 2.21E - 03, X_{tb} = 1.82, B_r = 3.40E - 01, I_{K_r} = 2.21E - 03, R_c = 1.43E + 02, C_{jc} = 3.68E - 14, M_{jc} = 0.333, V_{jc} = 0.700, C_{je} = 4.20E - 14, M_{je} = 0.560, V_{je} = .8950, T_r = 2.10E - 08, T_f = 6.98E - 11, I_{tf} = 2.25E - 02, V_{tf} = 1.34, X_{tf} = 12.31, R_b = 5.06E + 02, N_e = 2, I_{sc} = 0, F_c = 0.5$ |

obtained with $I_{B1} = 18 \mu A, I_{B2} = 4 \mu A, I_{B3} = 65 \mu A, I_{S1} = I_{S3} = 220 \mu A, I_{S2} = 240 \mu A$ and $C_1 = C_2 = 0.65$ nf. HPN was obtained with $I_{B1} = 65 \mu A, I_{B2} = 7.1 \mu A, I_{B3} = 10 \mu A, I_{S1} = I_{S3} = 220 \mu A, I_{S2} = 240 \mu A$ and $C_1 = C_2 = 0.65$ nf. The simulation results agree quite well with the theoretical analysis. Next, the Q tuning aspect of the circuit was verified for a constant pole frequency, for the BP response in CM. The bias currents I_{B3} and I_{S2} were varied simultaneously, by keeping its ratio to be constant. The Q variations, for constant pole frequency at 274 KHZ, are shown in Fig. 10. The Q is found to vary as 0.68, 1.75 and 3.55 for three values of $I_{B3} = I_{S2} = 40, 100$ and $200 \mu A$, respectively, which is greater than the theoretical value. This discrepancy is quite justifiable with the discussion of (39) in Section 4.1. The other design values were $I_{B1} = I_{B2} = 30 \mu A, I_{S1} = I_{S3} = 90 \mu A$ and $C_1 = C_2 = 0.65$ nf. Fig. 11 shows the variations in pole frequency with respect to I_{S2} , without affecting the bandwidth of the filter. The bias current I_{S2} was varied as 100, 200 and $400 \mu A$ and the pole frequency for a constant bandwidth at 950 KHZ is found as 685, 974 and 1.26 MHz, respectively, which is less than the theoretical value. This discrepancy is quite justifiable with the discussion of (38) in Section 4.1. For this result other design values were chosen as $I_{B1} = I_{B2} = I_{B3} = 60 \mu A, I_{S1} = I_{S3} = 220 \mu A$ and $C_1 = C_2 = 0.65$ nf. Further simulations were carried out to

verify the total harmonic distortion (THD). The circuit was verified by applying a sinusoidal current (I_{in}) of varying frequency and amplitude of $70 \mu A$. The THD values measured at the HP output (I_1) are found to be less than 3% while frequency is varied from 5 to 60 MHz. Moreover, the circuit was also simulated for THD analysis at HP output (I_1), by applying sinusoidal current (I_{in}) of varying amplitude and constant frequency. The THD values at frequency of 10 MHz are shown in Fig. 12, which clearly shows that for the input signal less than $180 \mu A$, the THD values remain in moderate range, that is, 3%. The Monte-Carlo analysis of the proposed

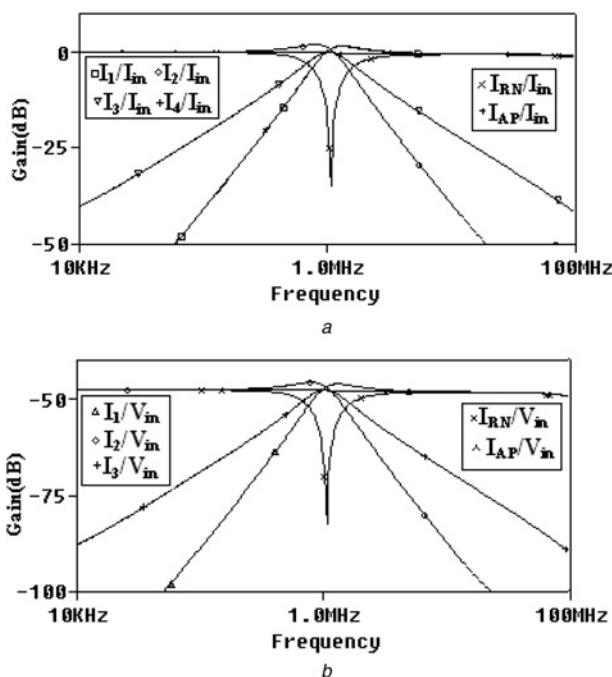


Fig. 5 Simulated gain responses of LP, BP, HP, RN and AP of the circuit in Fig. 3

- a In current mode
- b In trans-admittance mode

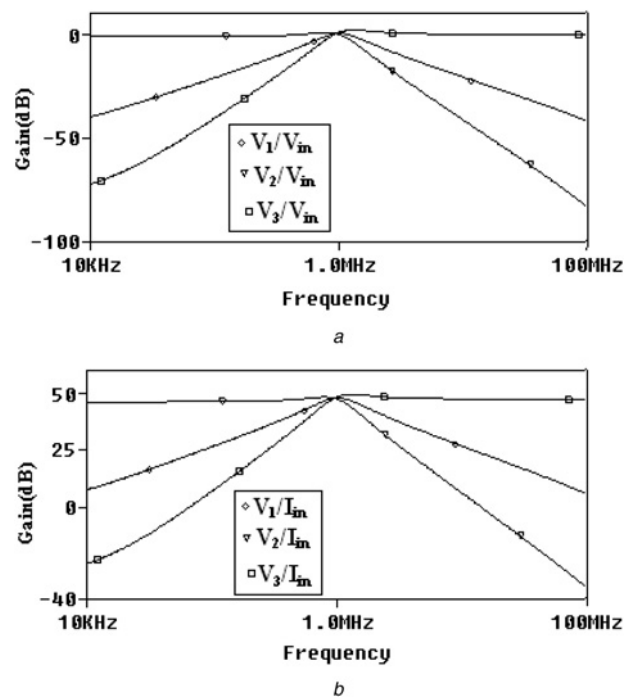


Fig. 6 Simulated gain responses of LP, BP and HP of the circuit in Fig. 3

- a In voltage mode
- b In trans-impedance mode

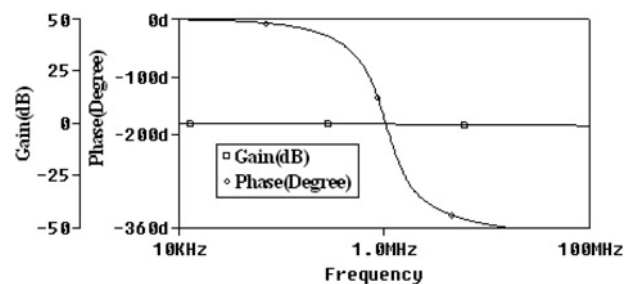


Fig. 7 Current gain and phase response of AP filter of circuit in Fig. 3

Table 4 Dependence of frequency deviation on $I_{B3}(R_{X3})$ for BP filter in current-mode

| $I_{B1}, \mu A$ | $I_{B2}, \mu A$ | $I_{S2}, \mu A$ | $I_{B3}, \mu A$ | Calculated(ideal) value of pole frequency, MHz | Simulated value of pole frequency, MHz |
|-----------------|-----------------|-----------------|-----------------|--|--|
| 60 | 60 | 240 | 60 | 1.134 | 1.06 |
| 60 | 10 | 240 | 10 | 1.134 | 1 |
| 60 | 1 | 240 | 1 | 1.134 | 0.854 |
| 60 | 0.1 | 240 | 0.1 | 1.134 | 0.832 |

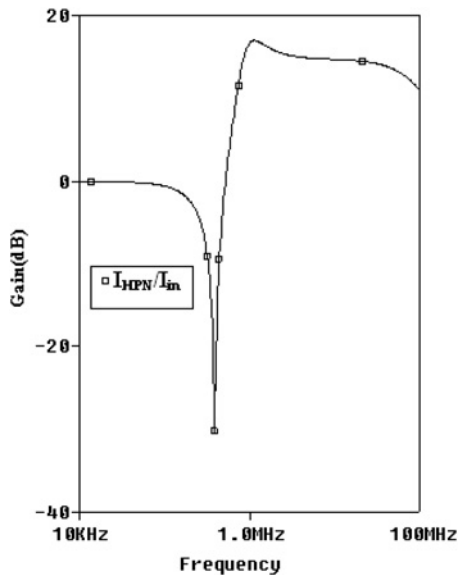


Fig. 8 Gain response of CM HPN of filter circuit in Fig. 3

circuit for $C_1 = C_2 = 0.65$ nf was next performed taking 10% tolerances in the capacitive components. The analysis was done for six runs. The time-domain response of BP output (I_3) in CM ($V_{in} = 0$) is shown in Fig. 13. It is observed that 50 μA peak-to-peak input current sinusoidal signal levels having frequency 1.06 MHz are possible without significant distortions. The results of Fig. 13 show the deviations in BP output for the above-mentioned tolerances in capacitive elements. BP output was chosen for presentation of the results, as the effect of capacitive deviations would alter the

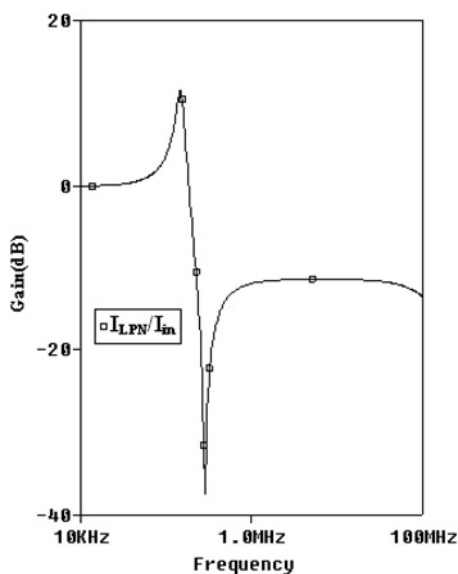


Fig. 9 Gain response of CM LPN of filter circuit in Fig. 3

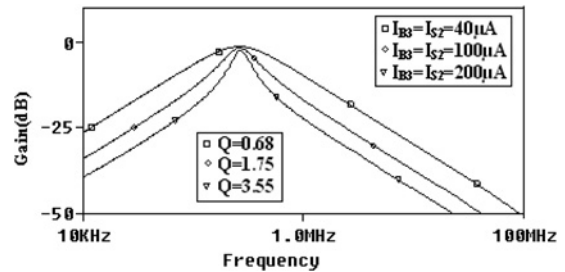


Fig. 10 BP responses in CM, for different values of $I_{B3} = I_{S2}$

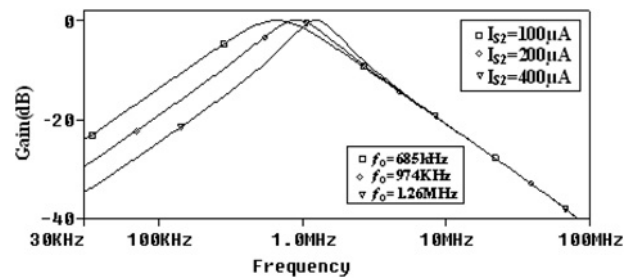


Fig. 11 BP responses in CM, for different values of I_{S2}

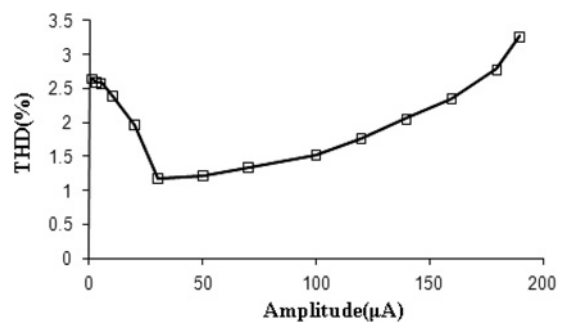


Fig. 12 Variation in THD at CM HP output (I_1) with input current signal at 10 MHz

centre frequency and the BP gain would be changed at the designed input frequency, but as seen from the Monte-Carlo analysis, the capacitive tolerances do not severely affect the circuit performance.

6 Possible experimental setup

It may be noted that the active building blocks like CCCII or CCCCTA have emerged as potential option for tunable circuit realisations. These are always better targeted for integrated circuit (IC) implementation rather than being built using off-the-shelf chips. However, repeated demands from the

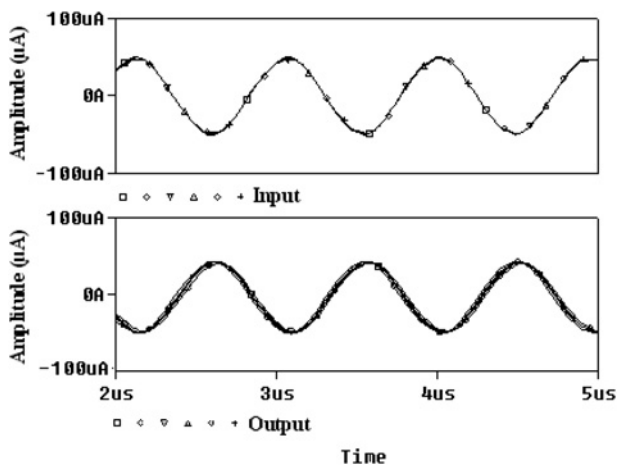


Fig. 13 Time-domain results of BP output for Monte-Carlo analysis

eminent knowledge providers often leads to innovative experimental setups, which may not be very feasible from the point of view of circuit complexity. With this reasoning and criticism, the CCCCTA can also be built using commercially available chips, like AD844 s and LM13600. It is well known that an AD844 can realise a second generation current conveyor with additional buffered Z output and LM13600 is the standard single-output operational trans-conductance amplifier. Such a circuit realisation for CCCCTA would require external resistors to be employed at X terminals (inverting terminals) of AD-844, thus making the circuit non-tunable, which in itself goes against the theme of this paper. However, it does provide a possible solution to the criticisms related to the need of experimental setups. The above-discussed realisation for CCCCTA is shown in Fig. 14 for purely academic reasons.

Thus, the proposed mixed-mode filter shown in Fig. 3 employs a minimum of eight AD844 and three LM13600 ICs for the experimental setups. If we compare the proposed mixed-mode filter with the previously reported mixed-mode filter circuits [26–29] in terms of actual hardware requirements for the experimental setups, then it may be noted that implementations of each of the reported

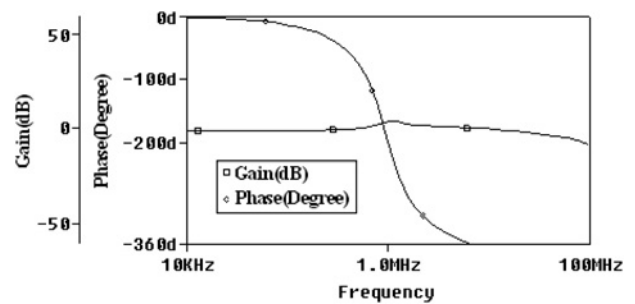


Fig. 15 Current gain and phase response of AP filter of circuit in Fig. 3, using AD844 and LM13600

circuits in [27–29] also requires an equal number or more ICs by way of being based on current conveyors with dual or multi-outputs. It may be noted that the implementation of a dual-output CCCII was recently given in [32]. The other reported circuit in [26] employs four AD844 ICs and switching arrangements for the experimental setups and need to be reconfigured for obtaining various responses unlike the proposed work. However, these comparisons are not really important if such circuits are targeted for IC implementations. Even though minimal complexity and power would still be of prime importance, Fig. 15 shows the gain and phase response of the CM AP using ICs AD844 and LM13600. The passive and active components value were chosen as R_{X1} ($I_{B1} = 60 \mu A$) = R_{X2} ($I_{B2} = 60 \mu A$) = R_{X3} ($I_{B3} = 60 \mu A$) = 216Ω , $I_{S1} = 220 \mu A$, $I_{S2} = 240 \mu A$, $C_1 = C_2 = 0.65 \text{ nf}$ and $V_{CC} = -V_{EE} = 5 \text{ V}$.

7 Conclusions

An electronically tunable low-voltage mixed-mode universal biquad filter using only three CCCCTAs and two grounded capacitors is proposed. The proposed filter offers the following attractive features:

1. Realises LP, BP and HP responses in four possible modes, from the same configuration.
2. The proposed circuit can also realise RN, LPN, HPN and AP in the current as well as trans-admittance-mode from the same topology.

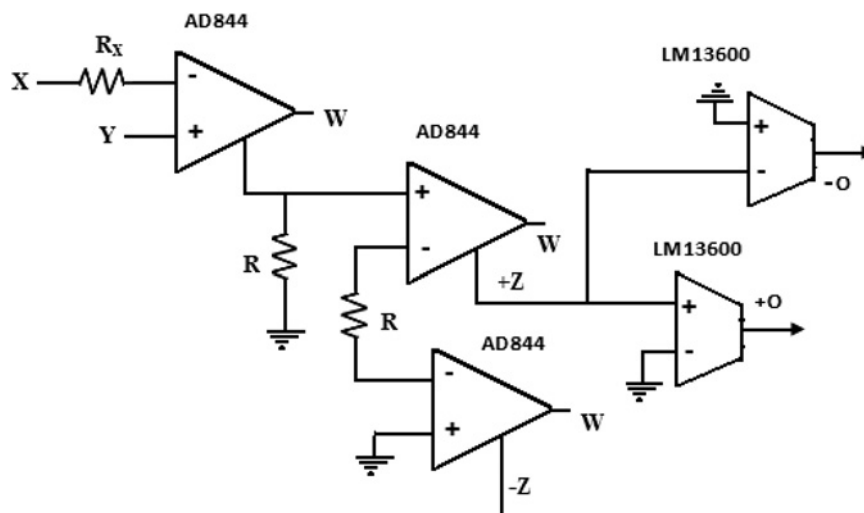


Fig. 14 Possible realisation of the CCCCTA using plus-type CCI (AD844) and OTA (LM13600)

3. Realises all the standard filter function in current and trans-admittance-mode at high output impedance which is suitable for easy cascading with next stage.
4. Use of only grounded capacitors makes the structure less sensitive to parasitic and easier to integrate.
5. Low sensitivity figures and low THD.
6. Low voltage supply of ± 1 V is required which makes the structure suitable for portable and battery powered equipments.
7. Filter parameters ω_o , Q , ω_o/Q and filter gains are electronically tunable with bias currents of CCCCTAs.
8. Simultaneous current control of ω_o and Q without disturbing of ω_o/Q .

With the above-mentioned features, it is very suitable to realise the proposed circuit in monolithic chip to use in modern microelectronic system applications, such as controls and voice and data communications, where consideration of size and weight makes the use of inductors prohibitive.

8 Acknowledgments

The authors are thankful to the anonymous reviewers for constructive criticisms and suggestions that helped to improve the paper. The author is also grateful to the Editor-in-Chief Professor Asim Ray for recommending the paper.

9 References

- 1 Wilson, B.: 'Recent developments in current-mode circuits', *IEE Proc. G*, 1990, **137**, pp. 63–67
- 2 Keskin, A.Ü., Biölek, D., Hancioglu, E., Biolkova, V.: 'Current-mode KHN filter employing current differencing transconductance amplifiers', *Int. J. Electron. Commun. (AEÜ)*, 2006, **60**, pp. 443–446
- 3 Soliman, A.M.: 'Current conveyor filters classification and review', *Microelectron. J.*, 1998, **29**, pp. 133–149
- 4 Senani, R., Singh, V.K.: 'KHN-equivalent biquad using current conveyors', *Electron. Lett.*, 1995, **31**, pp. 626–628
- 5 Biölek, D., Biolkova, V.: 'Three-CDTA current-mode biquad', *WSEAS Trans. Circuits Syst.*, 2005, **4**, pp. 1227–1232
- 6 Maheshwari, S.: 'Analogue signal processing applications using a new circuit topology', *IET Circuits Devices Syst.*, 2009, **3**, pp. 106–115
- 7 Soliman, A.M.: 'New current-mode filters using current conveyors', *Int. J. Electron. Commun. (AEÜ)*, 1997, **51**, pp. 275–278
- 8 Yuçe, E., Minaei, S., Cicekoglul, O.: 'Universal current-mode active-C filter employing minimum number of passive elements', *Analog Integ. Circuits Signal Process.*, 2006, **46**, pp. 169–171
- 9 Tsukutani, T., Sumi, Y., Yabuki, N.: 'Versatile current mode biquadratic circuit using only plus type CCCIs and grounded capacitors', *Int. J. Electron.*, 2007, **94**, pp. 1147–1156
- 10 Biölek, D.: 'CDTA-building block for current-mode analog signal processing'. Proc. ECCTD, Krakow, Poland, 2003, III, pp. 397–400
- 11 Wilson, B., Lidgey, F.J., Toumazou, C.: 'Current-mode signal processing circuits'. IEEE Proc. ISCAS'88, 1998, pp. 2665–2668
- 12 Maheshwari, S., Khan, I.A.: 'Novel cascadable current-mode translinear-C universal filter', *Active Passive Electron. Compon.*, 2004, **27**, pp. 215–218
- 13 Siripruchyanun, M., Jaikla, W.: 'Electronically controllable current-mode universal biquad filter using single DO-CCCDTA', *Circuits Syst. Signal Process.* 2008, **27**, pp. 113–122
- 14 Wu, J., El-Masry, E.: 'Current-mode ladder filters using multiple output current conveyors', *IEE Proc. Circuits, Devices Syst.*, 1996, **143**, pp. 218–222
- 15 Maheshwari, S.: 'High performance voltage-mode multifunction filter with minimum component count', *WSEAS Trans. Electron.*, 2008, **5**, pp. 244–249
- 16 Chang, C.M., Tu, S.H.: 'Universal voltage-mode filter with four inputs and one output using two CCII+s', *Int. J. Electron.*, 1999, **86**, pp. 305–309
- 17 Horng, J.W.: 'Voltage-mode universal biquadratic filter with one input and five outputs using OTAs', *Int. J. Electron.*, 2002, **89**, pp. 729–737
- 18 Singh, S.V., Maheshwari, S., Mohan, J., Chauhan, D.S.: 'An electronically tunable SIMO biquad filter using CCCCTA', *Contemp. Comput. CCIS*, 2009, **40**, pp. 544–554
- 19 Soliman, A.M.: 'Mixed-mode biquad circuits', *Microelectron. J.*, 1996, **27**, pp. 591–596
- 20 Abuelma'atti, M.T.: 'A novel mixed-mode current-controlled current conveyor-based filter', *Active Passive Electron. Compon.*, 2003, **26**, pp. 185–191
- 21 Abuelma'atti, M.T., Bentrica, A.: 'A novel mixed-mode CCII-based filter', *Active Passive Electron. Compon.*, 2004, **27**, pp. 197–205
- 22 Abuelma'atti, M.T., Bentrica, A., Al-Shahrani, S.M.: 'A novel mixed-mode current-conveyor-based filter', *Int. J. Electron.*, 2004, **91**, pp. 191–197
- 23 Abuelma'atti, M.T., Bentrica, A.: 'A novel mixed-mode OTA-C universal filter', *Int. J. Electron.*, 2005, **92**, pp. 375–383
- 24 Pandey, N., Paul, S.K., Bhattacharyya, A., Jain, S.B.: 'A new mixed-mode biquad using reduced number of active and passive elements', *IEICE Electron. Exp.*, 2006, **3**, pp. 115–121
- 25 Chen, H.P., Liao, Y.Z., Lee, W.T.: 'Tunable mixed-mode OTA-C universal filter', *Analog Integ. Circuits Signal Process.*, 2009, **58**, pp. 135–141
- 26 Singh, V.K., Singh, A.K., Bhaskar, D.R., Senani, R.: 'Novel mixed-mode universal biquad configuration', *IEICE Electron. Exp.*, 2005, **2**, pp. 548–553
- 27 Maheshwari, S., Khan, I.A.: 'High performance versatile translinear-C universal filter', *J. Act. Passive Electron. Devices*, 2005, **1**, pp. 41–51
- 28 Zhijun, L.: 'Mixed-mode universal filter using MCCCII', *Int. J. Electron. Commun. (AEÜ)*, 2009, **63**, (2), pp. 1072–1075
- 29 Lee, C.N., Chang, C.M.: 'Single FDCCII-based mixed-mode biquad filter with eight outputs', *Int. J. Electron. Commun. (AEÜ)*, 2009, **63**, (2), pp. 736–742
- 30 Siripruchyanun, M., Jaikla, W.: 'Current controlled current conveyor transconductance amplifier (CCCCTA): a building block for analog signal processing', *Electr. Eng.*, 2008, **90**, pp. 443–453
- 31 Senani, R., Singh, V.K., Singh, A.K., Bhaskar, D.R.: 'Novel electronically controllable current-mode universal biquad filter', *IEICE Electron. Exp.*, 2004, **1**, pp. 410–415
- 32 Maheshwari, S.: 'Current-mode third-order quadrature oscillator', *IET Circuits, Devices Syst.*, 2010, **4**, pp. 188–195